27
11.2.84 9Me (1)

DR-054

UCID--17271-84

DE85 000047

9
I-1780

E-DIVISION ACTIVITIES REPORT

Compiled by H. H. Barschall

July 1984

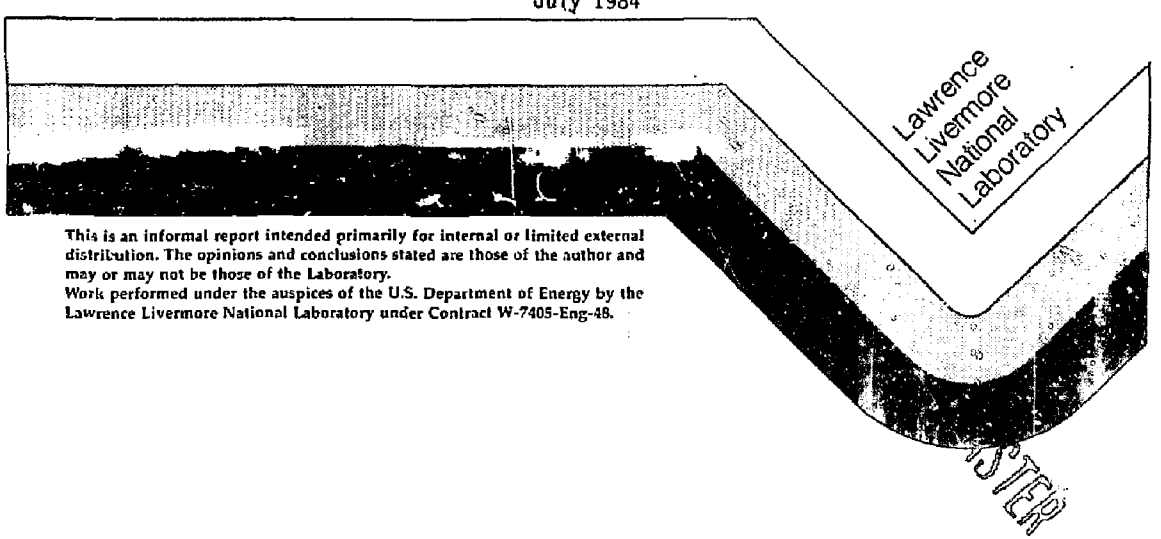

CONTENTS

E-Division Activities Report

July 1984

ABSTRACT

This report presents abstracts of papers published by E (Experimental Physics) Division staff members between July 1983 and June 1984. In addition, it lists the members of the scientific staff of the division, including visitors and students, and some of the assignments of staff members on scientific committees. A brief summary of the budget is included.

INTRODUCTION

E (Experimental Physics) Division carries out basic and applied research in atomic and nuclear physics, in materials science, and in other areas related to the missions of the Laboratory. Some of the activities are cooperative efforts with other divisions of the Laboratory, and, in a few cases, with other laboratories. Many of the experiments are directly applicable to problems in weapons and energy, some have only potential applied uses, and others are in pure physics.

E-Division has issued annual reports which describe some of the activities in the division during the preceding year. The last of these reports (UCID-17271-83) was issued in July 1983. Each of the previous reports gave brief descriptions of some of the research programs in the division. This portion of the annual report will be omitted this year. Instead abstracts of papers published since July 1983 are reproduced on the following pages.

The plan is to change the format of the annual report in the following years, but the details, including possible coordination with similar reports issued by other divisions of the Physics Department, have not yet been worked out.

LLNL published monthly in the ENERGY AND TECHNOLOGY REVIEW (UCRL-52000) descriptions of programs of general interest. Articles describing E-Division activities are reprinted in the E-Division annual reports. The following reprints were included in the previous reports:

Probing Nuclei with LLNL's Electron Linear Accelerator (1978)

RTNS: A Tool for Studying Neutron Damage (1978)

The Magnetic-Quadrupole Spectrometer: Studying Neutron Reactions (1978)

Pulsed Sphere Measurements for Weapons and Fusion Reactor Design (1978)

Measuring Hydrogen-Isotope Distribution Profiles (1978)

Nuclear Modeling at the LLL Cyclograaff (1979)

Studying Materials with Positrons (1980)

Probing Nuclear Structure with Electron Scattering Techniques (1980)

Channeling Radiation (1981)

ZAPP: A Facility for Studying Radiation from Hot, Dense Plasmas (1982)

Ozone, Respiration, and "The Bends" (1982)

Slow Positrons from the 100 MeV Linac (1982)

Ion Atom Interactions (1982)

ZAPP Upgraded (1983)

Joint U.S.-Japan Neutron-Source Program (1983)

How Old is the Universe? (1983)

Neutron Diagnostics for Magnetically Confined Plasmas (1983)

The present report includes:

Models of Nonequilibrium Nuclear Reactions

Intense Source of 14-MeV Neutrons

The RTNS-II Fusion Neutron Facility for Materials Damage Studies

D. W. Heikkinen and C. M. Logan

The Rotating Target Neutron Source (RTNS-II) is operated by Lawrence Livermore National Laboratory (LLNL) for the fusion energy programs of the U.S and Japan. Joint support and utilization by Japan (Monbusho) has been in effect since February 1982. The facility contains two identical neutron sources, each of which uses the $^{3}H(d,n)^{4}He$ reaction to generate 14-MeV neutrons. Deuteron beams in excess of 100 mA and 360 keV energy are incident on rotating tritium targets producing neutron source strengths $>2 \times 10^{13}$ n/s. A brief description of the neutron sources and their performance will be given. In addition, recent improvements in performance and reliability made possible by the additional funding from Japan are described. Finally, a short summary of the recent experimental program will be outlined.

Published in the Proceedings of the International Ion Engineering Congress, Kyoto, Japan, Vol. 1, p. 555 (1983).

Fission

THE $^{242}Am^{m}$ Fission Cross Section

J. C. Browne, R. M. White, R. E. Howe,
J. H. Landrum, R. J. Dougan, and R. J. Dupsyk

The neutron-induced fission cross section of $^{242}Am^{m}$ has been measured over the energy region from 10^{-3} ev to ~20 MeV in a series of experiments utilizing a linac-produced 'white' neutron source and a monoenergetic source of 14.1 MeV neutrons. The cross section was measured relative to that of ^{235}U in the thermal (0.001 to ~3 eV) and high energy (1 keV to ~20 MeV) regions and normalized to the ENDF/B-V $^{235}U(n,f)$ evaluated cross section. In the resonance energy region (0.5 eV to 10 keV) the neutron flux was measured using thin lithium glass scintillators and the relative cross section thus obtained was normalized to the thermal energy measurement. This procedure allowed a consistency check between the thermal and high energy data. The cross section data have a statistical accuracy of ~0.5% at thermal energies and in the 1-MeV energy region and a systematic uncertainty of ~5%. We confirmed that $^{242}Am^{m}$ has the largest thermal fission cross section known with a 2200 m/sec value of 6328 barns. Results of a Breit-Wigner sum-of-single-levels analysis of 48 fission resonances up to 20 eV are presented and the connection of these resonance properties to the large thermal cross section is discussed. Our measurements are compared with previously reported results.

Published in Physical Review C 29, 2188 (1984).

Measurement of the Prompt Fission Neutron Multiplicity from the $^{245}Cm(n,f)$ and $^{242}Am^{m}(n,f)$ Reactions

R. E. Howe, R. M. White, J. C. Browne, J. H. Landrum,
R. J. Dougan, R. W. Hougheed and R. J. Dupzyk

The prompt fission neutron multiplicity, $\bar{\nu}_p$, of ^{245}Cm was measured relative to that of ^{235}U using the neutron time-of-flight facility at the Lawrence Livermore National Laboratory (LLNL) 100-MeV electron linac. Incident neutron energies ranged from 0.05 eV to 14 MeV. In addition, a monoenergetic measurement of $\bar{\nu}_p$ for ^{245}Cm relative to ^{235}U was made at E_n = 14.1 MeV using the LLNL Insulated Core Transformer (ICT) Neutron Source. Fission fragments were detected using a hemispherical ionization chamber containing ~200 μg of ^{245}Cm. A separate fission chamber contained 8.3 mg of ^{235}U. Fission neutrons were detected in liquid scintillators using pulse-shape discrimination to separate gamma rays from neutrons. The measurements reported here for ^{245}Cm are in agreement with each other and indicate an overall rate of increase in $\bar{\nu}_p$ with incident neutron energy which departs significantly from systematic trends. Interpretations are presented which suggest that these results are a consequence of changing fragment kinetic energies. Results from a concurrent measurement of $\bar{\nu}_p$ for $^{242}Am^{m}$ at E_n = 14.1 MeV are also included and agree with previously reported data.

Published in Nuclear Physics A407, 193 (1983).

Neutron Cross Section Measurements

Neutron Absolute and Total Cross Section Difference Measurements in the Mass-140 Region

H. S. Camarda, T. W. Phillips and R. M. White

We have used the Lawrence Livermore National Laboratory (LLNL) 100-MeV electron linac and neutron time-of-flight facility to measure precise neutron total cross sections in the mass-140 region for incident neutron energies of 3-60 MeV. We measured the absolute neutron total cross section of ^{140}Ce and the total cross section differences of ^{139}La-^{140}Ce, ^{141}Pr-^{140}Ce and ^{142}Ce-^{140}Ce. These cross section differences oscillate with energy. Optical model calculations have been performed which fit the ^{140}Ce total cross section well over the 3-60 MeV energy region. The ^{139}La-^{140}Ce and ^{141}Pr-^{140}Ce difference data were satisfactorily fit by small changes in the geometrical parameters of the potential. The ^{142}Ce-^{140}Ce data could not be fit by small changes in the geometry of the potential and we found that the changes required to achieve a satisfactory fit suggest that ^{142}Ce is either non-spherical or more easily deformed than ^{140}Ce. Using our final optical model parameters we calculated $\delta\langle r^2\rangle = {}^{A}\langle r^2\rangle - {}^{140}\langle r^2\rangle$ for the real part of the potential. The ^{139}La-^{140}Ce and ^{141}Pr-^{140}Ce optical model values of $\delta\langle r^2\rangle$ were in agreement with corresponding $\delta\langle r^2\rangle_q$ values calculated using muonic x-ray data. The value for ^{142}Ce-^{140}Ce was not.

Published in Physical Review C 29, 2106 (1984).

The $^{12}C(n,\alpha)$ Reaction and the Kerma Factor for Carbon at E_n = 14.1 MeV

R. C. Haight, S. M. Grimes, R. G. Johnson, and H. H. Barschall

Energy and angular distributions of α-particles from the bombardment of carbon foils with 14.1-MeV neutrons were measured with a magnetic spectrometer. The observations included α-particles with energies above 1 MeV emitted at angles between 19° and 135°. The cross section for α-particle emission obtained by integrating over emission angle was 402 ± 46 mb. From these data and from evaluations of the elastic and inelastic scattering cross sections a kerma factor (energy deposition) of 1.84 ± 0.16 x 10^{-9} cGy cm^2 was deduced. The present cross section for the $^{12}C(n,n'3\alpha)$ reaction is much lower than previous measurements.

Published in Nuclear Science and Engineering 87, 41 (1984).

Analysis of Nucleon Scattering on Tin Isotopes

Analysis of (p,p), (p,n), and (n,n) Scattering on the Even Tin Isotopes Using the Lane Coupled Equations

C. Wong, S. M. Grimes, and R. W. Finlay

(p,p), (p,n), and (n,n) scattering on ^{116,118,120,122,124}Sn have been analyzed employing the Lane coupled equations. The (p,n) measurements were made at E_p = 24.5 MeV, the appropriate energy at which to complement existing (p,p) measurements at 24.5 MeV and (n,n) measurements at 11 MeV. A search routine on the Lane coupled equations code yielded the complex isovector and isoscalar strengths from the simultaneous fitting of (p,p) and (p,n) data. These strengths have provided excellent fits to the (n,n) data on all five tin isotopes. The near constancy of the real and imaginary isovector strengths with A implies that the effects of channel coupling to the first 2^+ and 3^- states are either small or fairly uniform over the isotopic sequence. The implications of the Lane coupled equations with regard to the Coulomb correction on the imaginary optical potential are discussed.

Published in Physical Review C 29, 1710 (1984).

Precompound-Model Analysis of Photonuclear Reactions

M. Blann, B. L. Berman, and T. T. Komoto

A large body of photonuclear-reaction data has been compared with predictions of the hybrid-plus-evaporation model. The data are for monoenergetic photons of energy from 25 to 132 MeV on ^{16}O, Sn, Ce, Ta, and Pb targets, measured by the Saclay group. A quasideuteron absorption mechanism was assumed to give the primary excitation, and the hybrid-plus-evaporation model was used to predict the excitation functions, the neutron-emission widths and multiplicities, and the number of fast neutrons and protons emitted per absorbed photon versus photon energy for Sn, Ce, Ta, and Pb. The parameters used in the calculations were the global set recently selected for nucleon-induced reactions. The calculated results are in excellent agreement with the experimental data over the entire energy range. Additional experiments are suggested in order to make possible stricter tests of the precompound-decay models and to provide further information on the details of the primary excitation process.

Published in Physical Review C 28, 2286 (1983).

Global Test of Modified Precompound Decay Models

M. Blann and H. K. Vonach

A single parameter set was adopted for the hybrid and geometry dependent hybrid models. The nuclear density profile was modified for consistency with results of the Myers nuclear droplet model. Optical model parameters were modified to give better global results for inverse reaction cross sections in the precompound energy range up to 90 MeV. Two types of multiple precompound decay processes are defined, and the more important of the two is incorporated into the precompound decay formalism. This results in two to five orders of magnitude improvement in predicting ^{202}Hg(p,2p) and ^{202}Hg(p,2pn) product yields for proton energies up to 86 MeV. The global parameter set and formulation of this work is compared with (n,xn) and (n,p) spectra for 14 MeV incident neutrons, for (p,n) spectra with 18-90 MeV protons, and with (p,p') spectra for 39-90 MeV protons. The goemetry dependent hybrid model gives the better overall agreement, in most cases within the 20-30% limit of significance attachment to the model. Some discussion is given of methods by which the calculations might be further improved.

Published in Physical Review C 28, 1475 (1983).

Precompound Evaporation Analyses of Excitation Functions for (α,xn) Reactions

M. Blann and T. T. Komoto

Calculated (α,xn) excitation functions (x = 1 to 4) for $^{233,234,235}U$ and ^{237}Np targets for incident ^{4}He energies to 45 MeV, have been compared with experimental results. Calculations used experimental fission barriers with single particle ratios which were deduced by fitting experimentally deduced fission probabilities at excitations up to 12 MeV. Standard precompound parameters used for fitting spectra of nucleon-induced reactions were used, changing only the initial exciton number to four, appropriate for α-induced reactions. Agreement with experimental results was good to excellent, without the need of multiple precompound decay, nor of variation of precompound decay parameters from those required for nonfissile systems.

Published in Physical Review C 29, 1678 (1984).

Precompound Analyses of $^{58\text{-}64}$Ni(n,px) Reactions

C. M. Castaneda, J. L. Ullmann, F. P. Brady, J. L. Romero,
N. S. P. King, and M. Blann

Data for the inclusive (n,px) reaction for 60 MeV neutrons on ^{58,60,62,64}Ni are presented. Angular distributions for Q-value bins show a decrease of the forward peaking of the proton emission with increasing neutron excess. A marked dependence of the angle integrated spectra on (N-Z) is observed. The data are compared to hybrid and geometry dependent hybrid model calculations. Although these results predict the general shape of the spectra, they do not account for (N-Z) dependence. A neutron skin, as given by a hydrodynamic model, is added to the geometry dependent hybrid model, which predicts a higher precompound decay for high impact parameters. These results agree much better with the (N-Z) dependence of the data.

Published in Physical Review C 28, 1493 (1983).

Measurements with Polarized Nucleons

Polarized Neutron Capture into ^{13}C: Evidence for a Secondary Doorway State Effect

J. G. Woodworth R. A. August, N. R. Roberson,
D. R. Tilley, H. R. Weller, and J. W. Jury

Angular distributions for the $^{12}C(n,\gamma_0)^{13}C$ reaction have been measured with neutrons corresponding to excitation energies of 16.0, 19.2, 20.1, 20.8 and 21.8 MeV. Legendre polynomial coefficients have been determined to second order (a_3 is small). Polarized neutron measurements were obtained at excitation energies of 16.0, 18.6, 19.2, 20.1, 21.0, 21.8 and 22.3 MeV. A structure seen in the coefficient of the Legendre polynomial P_2 for the $^{12}C(p,\gamma_0)^{13}N$ reaction is also seen in the present data. A secondary doorway state at 20.5 MeV with an apparent width of 0.5 MeV is suggested by previously measured $^{11}B(d,\gamma_0)^{13}C$ data. The presence of this state provides an explanation for the energy dependence of the cross section, the a_2 coefficient and the analyzing power coefficient b_2 in the $^{12}C(n,\gamma_0)^{13}C$ data. The same model is also able to describe the energy dependence of the cross section and the a_2 coefficient observed in the $^{12}C(p,\gamma_0)^{13}N$ reaction in the region of 16 to 22 MeV.

Published in Physical Review C 29, 1186 (1984).

Microscopic Analysis of $^{6}Li(\vec{p},p)g.s.$ and $^{6}Li(\vec{p},p')$ (2.18 MeV) Analyzing Powers at 25, 35, and 45 MeV

C. H. Poppe, F. S. Dietrich, D. Rowley, H. E. Conzett, D. Eversheim and C. Rioux

In the limit of the plane-wave Born approximation, analyzing powers for proton inelastic scattering result from interference between the central and spin-orbit parts of the effective nucleon-nucleon interaction. Because the real part of the effective spin-orbit interaction is generally much greater than its imaginary part, one expects that the analyzing powers should exhibit a sensitivity to the imaginary part of the effective central interaction. The presence of distortion in the entrance and exit channels modifies this conclusion somewhat, however for certain specific transitions this sensitivity is still maintained.

To test this hypothesis we have measured analyzing powers for proton scattering to the ground state (1^{+}; T = 0) and first excited state (3^{+}; T = 0) of ^{6}Li at the LBL 88 in. cyclotron. ^{6}Li was chosen because a recent study of the Li isotopes described successfully various (p,p') and (p,n) cross sections in terms of a realistic effective force, however analyzing powers were not treated. In the present work, inelastic analyzing powers and cross sections are compared to Born approximation calculations which use the density-dependent complex central interaction of Brieva and Rook and the real spin-orbit and tensor interactions of Elliott. Knockout exchange amplitudes are included in the calculation in the factorization approximation. Transition densities are derived from the Cohen-Kurath p-shell wave functions suitably modified to reproduce measured B(E2) values. The

effect of distortion on the calculations is studied for three different optical potentials -- two microscopic potentials based on the folding model of Jeukenne, Lejeune and Mahaux and a phenomenological model derived from previous fitting of elastic data. The predictions of these three potentials for elastic analyzing powers are also compared to the present elastic data.

Agreement between the analyzing power data and the calculations is not very good for either the ground or first excited state, indicating some serious deficiency in the model.

Published in The Interactions Between Medium Energy Nucleons in Nuclei (H. O. Meyer, Editor) p. 226, American Institute of Physics (1983).

Proton- and Alpha Particle-Induced Reactions

Charge Exchange (p,n) Reactions to the Isobaric Analog States of High Z Nuclei: $73 \leq Z \leq 92$

L. F. Hansen, S. M. Grimes, C. H. Poppe, and C. Wong

Differential cross sections have been measured for the (p,n) reaction to the isobaric analog states (IAS) of ^{181}Ta, ^{197}Au, ^{209}Bi, ^{232}Th, and ^{238}U at an incident energy of 27 MeV. Because of the importance of collective effects in this mass region, coupled-channel calculations have been carried out in the analysis of the data. Optical potentials obtained from the Lane model for the charge exchange reaction have been used in the simultaneous analysis of coupled proton and neutron channels. The sensitivity of the calculations to the different couplings between the levels and to the magnitude of the isovector potentials, V_1 and W_1, is discussed. The good agreement obtained between the measured and calculated (p,n) angular distributions to the analog state confirms the validity of the Lane formalism for high-Z nuclei ($Z \geq 50$). Elastic neutron differential cross sections inferred from the coupled-channel analysis are compared with measurements available in the literature in the energy range 7-8 MeV. The results of these calculations agree with the measured values as well as the results of calculations made using global neutron optical potential parameters optimized to fit neutron data.

Published in Physical Review C 28, 1934(1983).

Double Differential Cross Sections for (p,xn) Reactions of ^{64}Zn, ^{65}Cu and ^{89}Y with 26 MeV Protons

W. Scobel, L. F. Hansen, B. A. Pohl, C. Wong and M. Blann

Double differential cross sections for the inclusive production of neutrons from ^{64}Zn, ^{65}Cu and ^{89}Y bombarded with 26.0 MeV protons have been measured with time-of-flight techniques. The data reduction is discussed with respect to the influence of background corrections in the continuous part of the spectra, and a short comparison with preequilibrium model calculations is presented, showing good agreement with predictions of both the hybrid and the geometry-dependent hybrid model including multiple particle emission. The question of how to treat pairing remains open.

Published in Zeitschrift für Physik A311, 323(1983).

(α,n) and Total α-reaction Cross Sections for ^{48}Ti and ^{51}V

H. Vonach, R. C. Haight, and G. Winkler

The ^{48}Ti(α,n)^{51}Cr and ^{51}V(α,n)^{54}Mn cross sections were measured in the energy range 6-13 MeV to an accuracy of about 3%. The activation method was used for the determination of the reaction yields, and the product of incident flux and target thickness was determined from measurements of Rutherford scattering. Using known information on the competing charged-particle emission and extensive statis ical model calculations, tne total reaction cross sections for α particles on ^{48}Ti and ^{51}V could be derived with similar accuracy. Especially at lower energies our results are considerably smaller than the predictions of the widely-used Huizenga-Igo optical potential and support the potential of McFadden and Satchler.

Published in Physical Review C 28, 2278 (1983).

Intranuclear Cascade and Fermi Breakup Calculations of ^{1}H- and ^{4}He-induced Reactions on Light Target Nuclei

A. Gökmen, G. J. Mathews, and V. E. Viola, Jr.

Mass, energy, and angular distribution data for fragments with $A \geq 6$ produced in intermediate-energy proton- and alpha-particle-induced reactions on ^{12}C and ^{16}O nuclei are compared with the results of an intranuclear cascade calculation followed by deexcitation of the residual nuclei via a Fermi breakup mechanism. In this latter step all possible particle-stable exit-channel states are included in the phase space available for decay. The shapes of the angular distributions are reproduced successfully by the calculation, even at relatively low bombarding energies (e.g., E_{α} = 60 MeV). The energy spectra are also reproduced qualitatively. The isobaric cross sections of fragments heavier than the target nucleus are underpredicted for alpha-particle-induced reactions, whereas the yields of fragments with A = 6 - 8 are overpredicted. The former discrepancy is attributed to the importance of alpha-particle breakup during the cascade while the latter may serve as a measure of the relative importance of statistical multibody breakup mechanisms.

Published in Physical Review C 29, 1606 (1984).

Gamow-Teller Strength Functions with the Lanczos Algorithm

S.D. Bloom

A review of calculations of GT (Gamow-Teller) strength functions using the Lanczos algorithm is presented for the nuclei ^{26}Mg, ^{54}Fe, ^{56}Fe, ^{58}Ni, ^{60}Ni, and ^{90}Zr. A comparison with experimental results is made in each case using the PMM (all cases) and Chung-Wildenthal (^{26}Mg only) Hamiltonians. The finding is that in general the agreement between the experimental and theoretical shapes ranges from good to excellent but the theoretical total strengths are too large by a factor of .45 to .55, the so-called GT quenching factor. The introduction of a limited set of 2p/2h parent-state correlations for Zr did not materially change this finding. However only a central force was used in all calculations presented here (except for ^{26}Mg) and it is possible that (for example) a tensor force in combination with more extended 2p/2h parent state correlations would lead to a highly dispersed GT strength for excitations in the region 15 Mev to 60 Mev or even higher, in consonance with the predictions of Arima and Bertstch and Hamamoto.

An important caveat issuing from the present work is the need to ensure the consistency of the parent and daughter shell model bases as otherwise an unphysical dispersal of the Fermi strength as well as an equally unphysical enhancement and displacement of GT strength to high excitation energies (E_x > 20 MeV) can occur.

Published in Progress in Particle and Nuclear Physics 11, 500 (1984).

Gamow-Teller Strength Function for ^{90}Zr: Effects of Spin and Isospin Exchange Forces, and Ground-State Correlations

G. J. Mathews, S. D. Bloom, and R. F. Hausman, Jr.

Shell-model calculations of the Gamow-Teller strength function for ^{90}Zr have been performed utilizing a realistic finite-range two-body interaction in a model space consisting of the 2p and 1g shells. The effects of admixtures of two-particle two-hole excitations in ^{90}Nb, mostly due to the spin and isospin exchange components of the nucleon-nucleon force, are discussed. Ground state correlations in ^{90}Zr are also added via seniority-zero two-proton excitations from the 2p shell into the $1g_{9/2}$ shell. With the correlations the Gamow-Teller strength function is in good agreement with the experimental results and accounts for essentially all of the observed dispersion of strength. The inclusion of these correlations does not, however, produce either a displacement of Gamow-Teller strength to higher excitation energies, or a significant change in the total strength. Thus, they cannot account for the observed Gamow-Teller quenching. The quenching factor derived by a comparison of our calculated results with experiment is 0.52.

Published in Physical Review C 28, 1367 (1983).

Excitation of Analogue Isovector Resonances Via the (n,p) Reaction at 60 MeV

F. P. Brady, G. A. Needham, J. L. Ullmann, C. M. Castaneda,
T. D. Ford, N. S. P. King, J. L. Romero, M. L. Webb,
V. R. Brown, and C. H. Poppe

The (n,p) charge-exchange reaction is used as a selective tool for studying T + 1 isovector excitations. Here, 60 MeV neutrons have been used to measure (n,p) spectra from a range of nuclei. For ^{6}Li and ^{7}Li, large components of ℓ = 1 dipole strength, not seen in photoneutron data, have been found at higher excitation. In the cases of ^{6}Li, ^{12}C and ^{16}O comparison with photonuclear and (d, ^{2}He) data indicates that most of the ℓ = 1 strength appears to be s = 0. Gamow-Teller (GT)-type transitions have been measured in ^{6}Li, ^{12}C and ^{28}Si and a measure of $v_{\sigma\tau}$, the isovector spin-dependent component of the effective nucleon-nucleon interaction, has been obtained at 60 MeV. In the Ni isotopes, increasing blocking of the GDR with N-Z is seen. A structure of substantial strength in ^{209}Bi(n,p)^{209}Pb, originally thought to be isovector quadrupole, may more probably be evidence of a $2\hbar\omega$ $\sigma\tau$-type excitation.

Published in Journal of Physics G 10, 363 (1983).

Microscopic Modeling

Microscopic and Conventional Optical Model Analysis of Fast Neutron Scattering from $^{54,56}Fe$

S. Mellema, R. W. Finlay, F. S. Dietrich, and F. Petrovich

Differential cross sections for elastic scattering of neutrons from $^{54,56}Fe$ have been measured at several energies in the 20-25 MeV region. The data have been analyzed both in terms of the standard phenomenological optical model, and in the framework of two different microscopic models based upon nuclear matter calculations using realistic nucleon-nucleon interactions and a local density approximation. Isospin consistency of the microscopic-model calculations was also tested by analyzing proton elastic differential cross section data in the same energy region, as well as both proton and neutron elastic analyzing power data. The microscopic calculations yield quite reasonable agreement with the data, even through they contain no free geometrical parameters. The quality of the results for the analyzing power data is particularly impressive, indicating that the very simple, density and energy-independent spin-orbit force used in the calculations is sufficient. The differences between the various models are clarified by examining the momentum-space representations of the potentials.

Published in Physical Review C 26, 2267 (1983).

Isovector Effects in Nucleon Inelastic Scattering in a Density-Dependent Folding Model

S. Mellema, R. W. Finlay, F. S. Dietrich, and F. Petrovich

Differential cross section data for inelastic proton and neutron scattering to the first 2^+ states in ^{54}Fe and ^{56}Fe at several energies in the 11-26 MeV range have been analyzed using a microscopic distorted-wave Born approximation model. The entrance- and exit-channel optical potentials and the transition form factors were calculated consistently in a folding model using a density-dependent interaction obtained from nuclear matter calculations based upon a free nucleon-nucleon interaction. These microscopic calculations yield reasonable agreement with the data. The model was used to determine the ratio of neutron and proton transition matrix elements M_n/M_p for these excitations.

Published in Physical Review C 29, 2385 (1984).

Isospin Dependence of the Microscopic Optical Model for Nucleon Scattering

F. S. Dietrich, R. W. Finlay, S. Mellema,
G. Randers-Pherson, and F. Petrovich

ABSTRACT

New experimental data for the elastic scattering of 7-24 MeV neutrons from ^{208}Pb are presented, and a microscopic folding model study of neutron and proton elastic scattering data for ^{208}Pb at energies below 60 MeV is made to examine the isospin dependence of an effective interaction derived from nuclear matter calculations. The model interaction is shown to be in reasonable accord with the data and an important observation on Coulomb corrections is made.

Published in Physical Review Letters 51, 1629 (1983).

Branching Ratio in the Decay of $^{7}Be^{*}$

G. J. Mathews, R. C. Haight, R. G. Lanier, and R. M. White

The branching ratio for ^{7}Be electron-capture decay to the first excited state in ^{7}Li has been measured by implanting a 20-MeV ^{7}Be beam into a silicon detector telescope and counting the subsequent γ-decays with well calibrated Ge(Li) detectors. A branching ratio of 10.7±0.2% was obtained. This value is in agreement with past measurements but does not agree with a recently reported measurement by a similar technique. Sources of uncertainties and implications for nuclear physics and astrophysics are discussed.

Published in Physical Review C 28, 879 (1983).

States in ^{205}Tl and ^{210}Pb

3291-keV $J^{\pi} = (25/2)^{+}$ Level in ^{205}Tl

J. A. Becker, R. G. Lanier, L. G. Mann, G. L. Struble,
K. H. Maier, L. E. Ussery, W. Stöffl, T. W. Nail,
R. K. Sheline, J. A. Cizewski, B. H. Erkkila, and J. Blomqvist

A $J^{\pi} = (25/2)^{+}$ isomer in ^{205}Tl has been observed using techniques of in-beam γ-ray spectroscopy and the $^{204}Hg(t,2n)^{205}Tl$ reaction. The decay scheme firmly establishes the yrast levels: $[J^{\pi}, E_x(keV)]$ $(11/2)^{-}$, 1484.02; $(15/2)^{-}$, 2054.57; $(17/2)^{-}$, 2394.18; $(19/2)^{-}$, 2551.56; and $(25/2)^{+}$, 3290.7. A candidate for a 12^{-} state in ^{204}Tl with the configuration $(\pi h_{11/2}^{-1}, \nu i_{13/2}^{-1})$ is identified.

Published in Physical Review C 29, 1268 (1984).

Electromagnetic Properties of Isomers in ^{210}Pb

D. J. Decman, J. A. Becker, J. B. Carlson,
R. G. Lanier, L. G. Mann, G. L. Struble, K. H. Maier,
W. Stöffl, and R. K. Sheline

The lifetimes and magnetic moments of the $J = 8^+$ and 6^+ isomers in ^{210}Pb have been measured using the gamma-ray perturbed angular distribution technique. The levels were populated with the $^{208}Pb(t,p)^{210}Pb$ reaction. The g-factors of the 8^+ and 6^+ states are found to be -0.312(8) and -0.321(15), respectively. The magnetic moment, $\mu = -1.42(7)\ \mu_N$ is deduced for the $2g_{9/2}$ neutron orbital. Lifetimes are 290(25) ns for the 8^+ state and 71(9) ns for the 6^+ state. We find $\langle g_{9/2}||M(E2)||g_{9/2}\rangle = -39(2)$ e fm^2 and an effective charge of 0.88(5) e for the $2g_{9/2}$ neutron orbital.

Published in Physical Review C 28, 1060 (1983).

Electron Scattering

Inelastic Electron Scattering from ^{9}Be

R. W. Lourie, W. Bertozzi, T. N. Buti, J. M. Finn,
F. W. Hersman, C. Hyde, J. Kelly, M. A. Kovash, S. Kowalski,
M. V. Hynes, B. E. Norum, and B. L. Berman

The electromagnetic form factors have been measured for the lowest two $T = 3/2$ states in ^{9}Be at 14.393 and 16.976 MeV, the positive-parity state at 17.490 MeV, and a level of previously unknown J^{π} at 16.671 MeV. The range of effective momentum transfer is $0.9 \leq q_e \leq 2.5$ fm^{-1}. The data for the $T = 3/2$ states show considerable deviation from the results of intermediate-coupling shell-model calculations. In particular, for $q_e \leq 1.5$ fm^{-1}, where the M1 multipole dominates, the data lie well above these calculated values. There is some evidence that the state at 16.671 MeV has positive parity. The results of single-particle shell-model and Nilsson-model calculations are compared with the data for this state. The experimental form factor for the 17.490-MeV state can be fitted with single-particle shell-model results in the 2s-1d space.

Published in Physical Review C 28, 289 (1983).

Relativistic Heavy Ions

Factorization of Fragment-Production Cross Sections in Relativistic Heavy-Ion Collisions

D. L. Olson, B. L. Berman, D. E. Greiner,
H. H. Heckman, P. J. Lindstrom, and H. J. Crawford

Analysis of the factorizability of several sets of fragment-production cross sections has been performed for ^{12}C, ^{16}O, ^{18}O, and ^{56}Fe projectiles in the 1 to 2 GeV/nucleon energy region for targets ranging from Be to U. The results of this analysis are considered in terms of geometrical concepts. No evidence is found that there is any dependence of fragmentation channel upon the impact parameter. It is found that the projectile dependence of the target factors is much less than that predicted by the abrasion-ablation theory, and also is less than that predicted by an excitation-decay model. Nevertheless, it appears that an excitation and decay mechanism is the dominant process in peripheral fragmentation.

Published in Physical Review C 28, 1602 (1983).

Stopping Powers

α-Particle Stopping Power for Titanium and Vanadium

R. C. Haight and H. K. Vonach

A method for accurate measurement of the specific energy loss (dE/dx) of α-particles is described and results are given for titanium in the α-energy range 5.25 - 13 MeV and for vanadium in the range 5.25 - 12 MeV with uncertainties of about 3%. The results are in excellent agreement with the stopping power predictions of Ziegler and earlier precision measurements of the stopping power of protons and deuterons in Ti and V.

Published in Nuclear Instruments and Methods in Physics Research 81, 9(1984).

Nuclear Astrophysics

Synthetic H-R Diagrams as an Observational Test of Stellar Evolution Theory

G. J. Mathews, S. A. Becker and W. M. Brunish

Synthetic H-R diagrams are constructed from a grid of stellar models. These are compared directly with observations of young clusters in the LMC and SMC as a test of the models and as a means to determine the age, age dispersion, and composition of the clusters. Significant discrepancies between the observed ano model H-R diagrams indicate the possible influences of convective overshoot, large AGB mass-loss rates, and the best value for the mixing length parameter.

Published in Stellar Nuclearsyntheses (C. Chiosi and A. Reuzini, editors) p. 161, D. Reidel, Amsterdam, 1984.

Channeling Radiation

Planar and Axial Channeling Radiation from Relativistic Electrons in LiF

R. L. Swent, R. H. Pantell, H. Park, J. O. Kephart, R. K. Klein, S. Datz, R. W. Fearick, and B. L. Berman

Channeling radiation has been measured for planar-channeled 16.9-, 30.5-, and ∿54.3-MeV electrons and for axial-channeled 16.9-MeV electrons in the ionic crystal LiF. The results are shown to be in reasonable, but not perfect, agreement with calculations which model the crystal as an array of isolated Li^+ and F^- ions.

Published in Physical Review B 29, 52 (1984).

Comparison of Channeling Radiation from Diamonds With and Without Platelets

H. Park, R. H. Pantell, R. L. Swent, J. O. Kephart
B. L. Berman, S. Datz and R. W. Fearick

Channeling-radiation spectra produced by planar-channeled relativistic positrons and electrons in Type-Ia and Type-IIa diamonds have been measured. Because of the presence of platelets in the Type-Ia diamond, some of the spectra measured for this crystal differ markedly from their counterparts for the Type-IIa diamond. These striking differences illustrate the potential applications of channeling radiation as a diagnostic tool for studies of impurities or defects in crystals.

Published in Journal of Applied Physics 55, 358 (1984).

Channeling-Radiation Experiments

B. L. Berman and S. Datz

In the last five years, many of the properties of channeling radiation have been delineated experimentally. Channeling radiation is very intense, easily tunable, forward-directed, and for the planar case linearly polarized. Especially during the last two years, owing mainly to rapidly improving experimental techniques, there has been an explosive growth in the amount and quality of data that have been obtained. At this time, in fact, the data are sufficiently accurate to call into question the validity of the "standard" potentials used to describe well-known crystals, such as diamond. Also, measurements have been made which demonstrate the sensitivity of channeling radiation as a diagnostic probe of impurities and defects in crystalline materials.

Published in "Coherent Radiation Sources" (H. Überall and A. W. Saenz, Editors) Springer Verlag, Heidelberg (1984).

Time and Space Resolved Neutron Diagnostic Systems for Magnetically Confined Plasmas

D. R. Slaughter, H. S. Spracklen and R. Delvasto

Neutron spectrometer/counter systems have been developed for diagnostic measurements on magnetically-confined deuterium and deuterium-tritium plasmas. An early version was used to determine the mean ion energy as well as the ion-energy confinement time in the endplugs of the Tandem Mirror Experiments. A recent upgrade includes a 10 MHz pulse height analysis and particle identification capability for time- and space-resolved neutron spectrum measurements. Resolution is adequate for a neutron doppler-width measurement of mean ion energy in near-future confinement experiments such as the Mirror Fusion Test Facility.

Published in Nuclear Instruments and Methods 215, 443 (1983).

A Real-Time Neutron Beam Monitor

J. A. Becker

An array of multiwire proportional counters has been employed to image, in "real-time," a collimated neutron beam produced at an electron linac facility. Test results are presented, along with a discussion of the advantages of this technique.

Published in Nuclear Instruments and Methods 211, 297(1983).

Oxidation and Hydriding of Uranium Studied by Positron Annihilation

R. H. Howell, C. Colmenares, and T. McCreary

The oxidation of uranium by water vapor and dry or humid oxygen, and the hydriding of uranium by dry or humid hydrogen has been studied by positron annihilation measurements. Positron-lifetime and Doppler-broadening measurements exhibit features that are correlated with the reaction conditions and with the defect complexes controlling the reactions. There is evidence of positronium formation and trapping and specific lifetime values are associated with different defect complexes.

Published in Journal of Less Common Metals 98, 267(1984).

Positron Camera

P. K. Weathersby, S. S. Survanshi, and P. Meyer

Positron-emitting isotopes are becoming used more extensively in experimental and clinical medicine. Since most applications seek an image of the distribution of isotopes in the body, careful treatment of all spatial considerations is essential. These include treatments of inherent detector spatial response, attenuation and accidental coincidence, as well as a variety of transform and iterative reconstructions.

One of the earliest positron imaging devices is a pair of opposed gamma cameras operated in coincidence. Though more specific ring designs are now in use, a pair of stationary large area detectors continue to be quite functional and relatively inexpensive. In our use of such a device we encountered a number of problems in correcting for the spatial response of the camera. Other treatments of the response question do not produce a full or precise result. This report relays an exact geometric description of the spatial response function.

Published in Nuclear Instruments and Methods in Physics Research 220, 571 (1984).

Energy Flow in Magnetic Fusion Experiment

Energy Confinement Studies in the Tandem Mirror Experiment (TMX)

D. P. Grubb, S. L. Allen, T. A. Casper, J. F. Clauser,
F. H. Coensgen, R. H. Cohen, D. L. Correll, W. C. Cummins,
J. C. Davis, R. P. Drake, J. H. Foote, A. H. Futch, R. K. Goodman,
G. E. Gryczkowski, E. B. Hooper, Jr., R. S. Hornady, A. L. Hunt,
C. V. Karmendy, W. E. Nexsen, W. L. Pickles, G. D. Porter,
P. Poulsen, T. D. Rognlien, T. C. Simonen, D. R. Slaughter,
P. Coakley, G. A. Hallock, and O. T. Strand

Using the measured plasma densities and energies, the flow of power between the different particle species and regions of the tandem mirror experiment (TMX) is analyzed. The power flow is described by a simple classical model modified to include: (1) a halo of cool plasma that reduces end-cell ion losses due to charge exchange on background gas, (2) instability heating of the central-cell ions both in the central cell and as they escape through the plugs, (3) electron energy transport along the field lines which is less than predicted, and (4) radial transport of the central-cell ions. Our global power balance, including all particles and regions, accounts for 83 $\pm$ 27% of the trapped neutron-beam power.

Published in Physics of Fluids 26, 1987 (1983).

SCIENTIFIC STAFF

R. A. Alvarez, Ph.D., Stanford 1964
R. W. Bauer, Deputy Div. Leader, Ph.D., M.I.T. 1959
N. L. Back, Ph.D., Washington 1982
J. E. Bailey, Ph.D., U.C. Irvine 1984 (joined E-Division December 1983)
J. A. Becker, Ph.D., Florida State 1962
B. L. Berman, Ph.D., Illinois 1963
H. M. Blann, Ph.D., U.C. Berkeley 1960
S. D. Bloom (also Department of Applied Science, U.C. Davis)
Ph.D., Chicago 1952
R. Booth, B.A., San Jose State 1954
D. D. Dietrich, Ph.D., SUNY Stony Brook 1974
F. S. Dietrich, Ph.D., California Institute of Technology 1964
P. O. Egan, Ph.D., Yale 1975 (joined E-Division August 1983)
R. J. Fortner, Ph.D., Notre Dame 1968
R. C. Haight, Assoc. Div. Leader, Ph.D., Princeton 1969
L. F. Hansen, Ph.D., U.C. Berkeley 1959
D. W. Heikkinen, Ph.D., Iowa 1965
R. H. Howell, Ph.D., Michigan State 1972
T. T. Komoto, B.A., Fresno State 1956
C. M. Logan, M.S., U.C. Davis, 1972 (Mechanical Engineering Dept.)
R. E. Marrs, Ph.D., Washington 1975
G. J. Mathews, Ph.D., Maryland 1977
P. Meyer, M.S., Washington 1960
T. W. Phillips, Ph.D., M.I.T. 1967
B. A. Pohl, M.S., Michigan 1962
C. H. Poppe, Division Leader, Ph.D., Wisconsin 1962
I. D. Proctor, Ph.D., Michigan State 1972
I. J. Rosenberg, Ph.D., Brandeis 1980 (joined E-Division January 1984)
D. R. Slaughter, Ph.D., U.C. Berkeley 1973
R. E. Stewart, Ph.D., U.C. Davis 1983 (joined E-Division Sept. 1982)
R. M. White, Ph.D., Ohio 1977
C. Wong, Ph.D., California Institute of Technology 1953
J. G. Woodworth, Ph.D., Toronto 1978

R. C. Haight was elected Fellow of the American Physical Society.

Members of the staff served on several national committees:

American Physical Society

Committee on the Status of Women in Physics. L. F. Hansen

Committee on the International Freedom of Scientists.
L. F. Hansen

Department of Energy

Nuclear Data Committee. R. C. Haight

International Nuclear Data Committee. R. C. Haight,
Advisor and Chairman of Subcommittee B

Committee to Review Program to Provide Nuclear Data for
Fusion, Basic Energy Sciences. R. C. Haight

Panel for the Review of Nuclear Physics Research at the
Brookhaven High Flux Beam Reactor. B. L. Berman

National Research Council

Panel on Basic Nuclear Data Compilations. C. H. Poppe

Lawrence Berkeley Laboratory

Superhilac Executive Committee. H. M. Blann

Executive Committee of the 88 in. Cyclotron Users Association.
F. S. Dietrich

Members of the staff served on several conference committees:

Neutron Nucleus Collisions: A Probe of Nuclear Structure,
Glouster, OH, 5-8 Sept. 1984.
F. S. Dietrich, Program Committee, Organizing Committee
C. H. Poppe, Organizing Committee

Fifth International Symposium on Capture Gamma-Ray Spectroscopy
and Related Topics, Knoxville, TN. 10-14 Sept. 1984.
F. S. Dietrich, Program Advisory Committee

Conference on New Directions in Soft X-ray Photoabsorption,
Pacific Grove, CA. 8-11 April, 1984
R. J. Fortner, Organizing Committee

International Conference on Nuclear Data for Basic and Applied Science,
Santa Fe, NM. 13-17 May, 1985.
R. C. Haight, General Program Advisory Committee

LANL/LLNL Weapons Nuclear Physics Workshop, Livermore, CA.
25-27 Sept. 1984.
R. C. Haight, Co-chairman

CEBAF 1984 Summer Workshop, Newport News, VA. 25-29 June 1984.
B. L. Berman, Chairman of Working Group on Positron Beams

Fifth Topical Conf. on Atomic Processes in High Temperature Plasmas, Pacific Grove, CA, 25-28 Feb. 1985.
R. F. Fortner, Organizing Committee

R. C. Haight was a participant in the Coordinated Research Program of the IAEA on 14-MeV Neutron Nuclear Data for Fission and Fusion Reactor Applications.

Members of the staff were invited to give papers at national or international meetings.

NATO Advanced Research Workshop on Positron Scattering in Gases, 1983, London, England. "Intense Positron Beams: Linacs". R. H. Howell

Materials Research Society 1983 Annual Meeting, 1983, Boston, MA. "The Use of New Intense Variable-Energy Positron Sources". R. H. Howell

Fifth Riso International Sumposium on Metallurgy and Materials Science, 1983, Roskilde Denmark. "Characterization of High Energy Radiation Damage in Molybdenum". R. H. Howell

36th Annual Gaseous Electronics Conference, 1983, Albany, NY. "Air Breakdown by Short High-Power Microwave Pulses". R. A. Alvarez

International Ion Engineering Congress, 1983, Kyoto, Japan. "The RTNS-II Fusion Neutron Facility for Materials Damage Studies". D. W. Heikkinen

SNL Workshop on X-Ray lasers, 1984, Albuquerque, NM. "Laboratory Experiments Using Pulsed Power Generators". R. J. Fortner

Conference on New Directions in Soft X-Ray Photoabsorption, 1984, Pacific Grove, CA. "Atomic Processes in Dense Plasmas". R. J. Fortner

Students

D. L. Aron, B.S., U.C. Berkeley 1975

D. P. Byrne, B.S., Montana 1977

G. A. Chandler, B.S., SUNY Buffalo 1979

B. A. Dahling, B. S., U.C. Davis 1983

C. G. Foote, B.S., U.C. Davis 1975

S. S. McClure, B.S., California Polytechnic Institute 1983

T. J. Nash, B.S., Long Beach State 1977

D. L. Olson, B.S., Missouri 1975, Ph.D. U.C. Davis 1983

D. F. Price, B.S., North Carolina State 1978

B. K. Young, B. S., Hawaii 1980

Visiting Faculty Members (Consultants)

H. H. Barschall, Wisconsin

H. S. Camarda, Pennsylvania State

J. A. Carr, Florida State

J. A. Cizewski, Yale

T. W. Donnelly, M.I.T.

R. W. Finlay, Ohio

J. D. Garcia, Arizona

C. D. Goodman, Indiana

S. M. Grimes, Ohio

A. K. Kerman, M.I.T.

H. W. Le[illegible]e, Oregon

V. A. Mac[illegible]Oregon State

J. E. Merce[illegible]d, Caltech

F. L. Petrovich, Florida State

Guests Participating in Livermore Experiments

Ulrich K. Boesl, Stanford

Michael J. Fluss, Argonne

Theodor W. Hänsch, Stanford

James W. Jury, Trent (Canada)

Jon T. Larsen, KMS Fusion

Kenneth G. McNeill, U. of Toronto (Canada)

Richard H. Pantell, Stanford

Heungsup Park, Stanford

Melvin Piestrup, Stanford

Robert Pywell, Saskatchewan (Canada)

Richard L. Swent, Varian Associates

Maxwell N. Thompson, U. of Melbourne (Australia)

Matthias Trabandt U. of Hamburg (West Germany)

Herbert Vonach, Vienna (Austria)

Draghish Zubanov, U. of Melbourne (Australia)

Outside Users of RTNS-II Facility

ANL:	R. Smither
BNL:	C. Snead
HEDL:	C. Cannon H. Heinisch
Hiroshima:	Y. Shimomura
Hokkaido:	M. Kiritani H. Takahashi
Kyoto:	C. Ichihara Y. Yamaoka H. Yoshida
Kyushu:	T. Kinoshita E. Kuramoto K. Shinohara N. Yoshida
LANL:	J. Fowler
Nagoya:	M. Iseki N. Itoh H. Kamada K. Sata
Osaka:	T. Okada K. Sumita
TIT:	K. Kawamura K. Saneyoshi
Tohoku:	K. Abe H. Kayano H. Matsui K. Okamura K. Suzuki
Tokoyo:	M. Doyama N. Igata S. Ishino H. Kawanishi A. Kohyama K. Miyahara Y. Tabata
Vienna:	P. Hahn

APPENDIX

Models of Nonequilibrium Nuclear Reactions

Simple multiple scattering models of the nuclear reaction mechanism enable us to include nonequilibrium effects in our calculations of important but unmeasurable nuclear cross sections.

For further information contact Marshall Blann (415) 422-4515.

Nuclear modeling attempts to describe mathematically the many things that can happen to an atomic nucleus when it is struck by a subatomic particle such as a neutron or proton. Nuclear modeling helps us to understand the various mechanisms by which nuclear reactions take place and, therefore, how the effects of these mechanisms vary with target, projectile, and projectile energy.[1] To the degree that researchers have achieved such an understanding, they can predict the differential and integral cross sections for any nuclear reaction of interest (see box on p. 13).

Equilibrium thermodynamics is a powerful tool for such nuclear modeling, but it cannot be applied in a straightforward manner to nonequilibrium phenomena (the subject of this article), which must be included if modeling is to produce quantitatively accurate results. Solutions to the problem of modeling nonequilibrium mechanisms have been elusive, but considerable progress has been made with simple models based on the concept that these reactions proceed through a series of nucleon-nucleon scattering processes inside the nucleus.[2] With some extensions, these models have reproduced quite successfully a large body of experimental data.

The significance of these advances in nuclear modeling rests on the crucial need, in many fields, to predict the cross sections for a variety of nuclear reactions. In weapons testing, for example, determining radiochemical yield is vital. Many of the cross sections needed to interpret the data cannot be measured experimentally because they involve unstable target isotopes. Fission-reactor neutronics involve very large numbers of cross sections, too numerous to measure. In other fields, such as medicine or industry, there is often the need to answer questions about how best to produce a particular isotope. In all such cases, nuclear modeling attempts to provide the answer.

Nuclear modeling is of interest at LLNL for its present and potential applications in laser fusion, mirror fusion, and weapon design. Scientists at the Laboratory have refined the nonequilibrium model and the codes used to implement it, and LLNL experimentalists have provided a unique set of data that has enabled us, for the first time, to test the model over a broad range of energies.

In this article, we briefly review the equilibrium reaction mechanism (which determines a large part of the reaction cross sections) as well as the more recently treated nonequilibrium reaction mechanisms. We then describe the very simple modeling approaches that have been so successful in explaining the part of the particle yield produced by nonequilibrium reactions.

Mechanisms for Fast Nucleon Reactions

Figure 1 compares the experimental results and calculations of capture and reemission of 14-MeV neutrons by iron-56 (14-MeV neutrons are the main byproduct in D-T fusion reactions). The shape of the spectrum is analogous to that of the energy distribution of molecules evaporated from a fluid surface. The nuclear model for treating this phenomenon, called the compound-nucleus or evaporation model, dates back to early work by Niels Bohr.[3]

The evaporation model is one of the most widely used and successful reaction models. Particle-emission spectra may be characterized by a temperature, completing the analogy with the fluid evaporation process. The first formulation of this model for nuclear reactions was made by Weisskopf.[4] Although more sophisticated formulations have been made,[5] Weisskopf's equation is still widely used. The calculated differential spectrum shown in Fig. 1 is based on this model and gives an excellent description of the experimental results over most of the energy range of the emitted neutrons, with the largest discrepancies occurring only at high energies.

Nonequilibrium Component

When we consider the reaction of 14-MeV neutrons on a niobium-93 target,[6] however, we see that the prediction based on the pure evaporation model of the neutron spectrum breaks down even more in the high-energy portion of the spectrum (see Fig. 2). This deficiency in the evaporation model was noted in

Fig. 1

Spectrum of neutrons (differential cross section vs energy) from iron-56 bombarded by 14-MeV neutrons. Points with error bars represent yields from sources cited in Ref. 6; the yellow curve is the prediction calculated using a pure evaporation model.

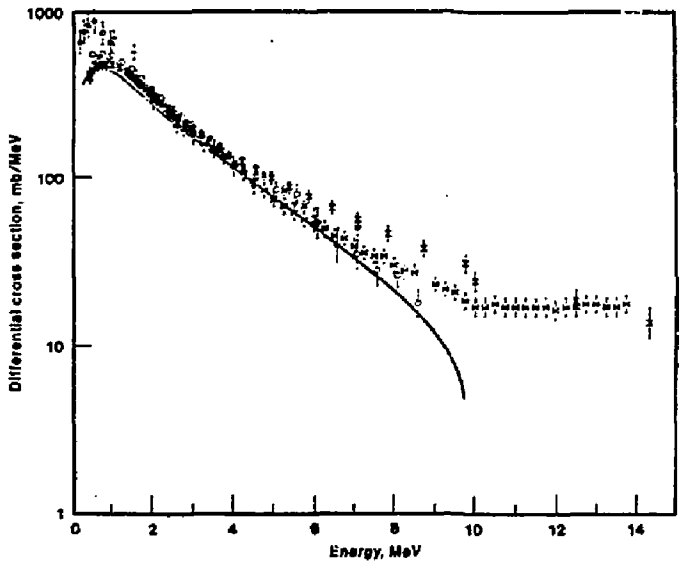

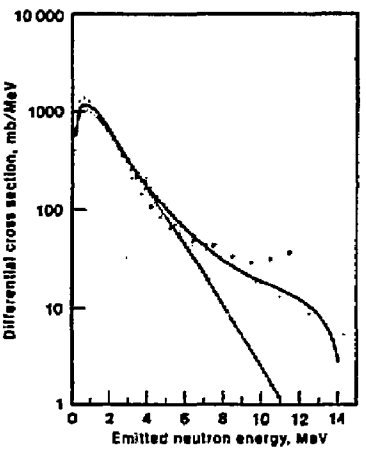

Fig. 2

Experimental and theoretical neutron-emission cross sections from bombardment of niobium-93 with 14-MeV neutrons. This figure is from Ref. 6, which also contains references to the data sources. The predictions of a pure evaporation model are shown in yellow; predictions of a pre-compound model plus the evaporation model are shown in black.

many experiments involving differential particle spectra and in the Laboratory's pulsed sphere program.[7] Does this deficiency come from a different reaction mechanism, or do we need merely to adjust the parameters of the evaporation calculation to force a fit to the data? This question bears directly on the correctness of the physics in our models.

To investigate this question, we need to study how the spectral distributions change as we increase the energy of the incident particle. The evaporation model does not treat any processes occurring between the time the incident particle enters the nucleus and the time thermal equilibrium is achieved (i.e., the condition under which the compound-nucleus/evaporation model may be applied). This assumption works well at projectile energies below approximately 14 MeV, but it becomes increasingly unrealistic at higher energies.

There is a slight difficulty in that well-collimated, intense, monoenergetic neutron beams for studying reactions generally are not available. Fortunately, however, protons may be substituted for neutrons in investigations of this kind.[8] The important difference involves the Coulomb barrier, and we understand quite well how to correct for this. Proton beams of high quality and intensity and a wide range of energies are readily available from modern accelerators.

Varying the projectile energy has effects on particle-emission spectra; Fig. 3 shows the spectra of protons reemitted from iron-54 following bombardment by incident protons of 29, 39, and 62 MeV.[9] The evaporation component (the broad peak centered at around 5 MeV) is relatively invariant with increasing projectile energy. This indicates that the evaporation model is valid where it applies, and its parameters should not be changed.

The excessive number of high-energy protons that are emitted continues to grow with increasing projectile energy. At an incident proton energy of 62 MeV, it has become the single most important contribution to the emission spectrum. For this and other more fundamental reasons, we must understand the mechanism by which this component originates.

The evaporation model is based on the assumption that the projectile is captured by a relatively "black" (i.e., totally absorbing) nucleus and that this capture leads to a fully equilibrated, compound system in which a large number of nucleons share the available excitation energy (Fig. 4a). Although a projectile can travel across the nucleus in 10^{-22} s, a compound nucleus takes a thousand to ten million times longer before it reemits particles. Perhaps the

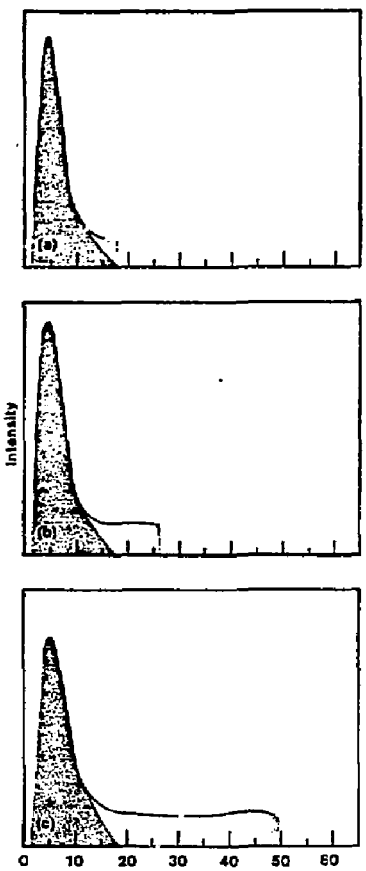

Fig. 3

Inelastic spectra for iron-54 (p,p') at 35° for incident proton energies of 29 MeV (a), 39 MeV (b), and 62 MeV (c). The peak predicted by the evaporation model (dark gray) fits the low-energy data well, but the high-energy portion associated with the precompound effects (yellow) becomes more and more prominent. Data are from Ref. 9.

high-energy component of the cross sections can be traced to the process by which the nucleus reaches thermal equilibrium.

Reactions induced by very energetic nucleons (more than 100 MeV) have long been treated as if the nucleus were a bag of marbles and the projectile yet another marble shot into the pack (represented schematically in Fig. 4b). From this concept comes the intranuclear cascade model, which is based on the idea that the incident particle transfers its energy to individual nucleons in successive nucleon-nucleon scattering events. In this model, the multiple scattering (called an "intranuclear cascade") is calculated in three-dimensional geometry by the laws of classical mechanics.[6] The process is calculated until one or more of the particles leave the nucleus or until there have been enough scattering events to distribute the incident particle's energy randomly among a large number of excited nucleons. The computations are lengthy but have been quite successful for reactions induced by projectiles having energies above 100 MeV.

Low-Energy Reactions

It was thought that the concept of excitation transport by successive two-body (nucleon-nucleon) collisions could not be applied to excited nucleons of lower energy since, as nuclear energy decreases, the expectation of well-defined nucleon-nucleon collisions becomes harder to justify. The reason for this is that the positions of individual nucleons cannot be specified more precisely than their reduced deBroglie wavelengths, and the latter become relatively large at lower energies. This enlargement leads to the possibility that each interaction of the projectile may simultaneously involve several nucleons rather than only one. Furthermore, the refractive properties of low-energy nucleons are difficult to treat in the classical scattering approximation illustrated in Fig. 4b; this difficulty stems from the problem of representing the scattering trajectories geometrically.

Fig. 4

Schematic representation of two different models for a nuclear reaction. (a) The evaporation model, which considers the nucleus a homogeneous black sphere capable of absorbing an incident particle and distributing its energy before other reactions take place, and which is reasonably successful in describing low-energy reactions. (b) The high-energy model (100 MeV or more) considers the nucleus a bag containing neutron and proton fermions; it uses a three-dimensional geometric representation to follow trajectories for successive two-body scattering processes; one such collision is shown in this figure.

Nuclear Cross Sections

Nuclear reactions take place on such a small scale that they cannot be observed directly. Instead, we observe large numbers of them and treat the results statistically. Instead of saying, "This particle will strike this nucleus and produce this effect," we can only say "This kind of particle, striking this kind of nucleus, has such and such a probability of producing this effect."

If we think of the protons and neutrons as unaimed bullets and the nuclei as spherical targets, it is natural to describe the probability of any particular interaction in terms of the target's cross-sectional area. The larger the target's cross section, the better its chance of being struck. The common unit of cross section is the barn (b), from the expression "hitting the broad side of a barn"; 1 b equals 10^{-28} m^2.

The total cross section for each nuclear reaction is a function of the energy of the incident particle. This does not mean that the nucleus changes size, but simply that the reaction is more likely to occur for certain particle energies than for others.

Following excitation by the projectile, the nucleus may decay (e.g., by emitting one or more particles or gamma rays). If 30% of the nuclei emit one neutron, for example, then the integral cross section for neutron emission would be 30% of the total reaction cross section. The differential cross section expresses the probability that neutrons of some particular energy will be emitted.

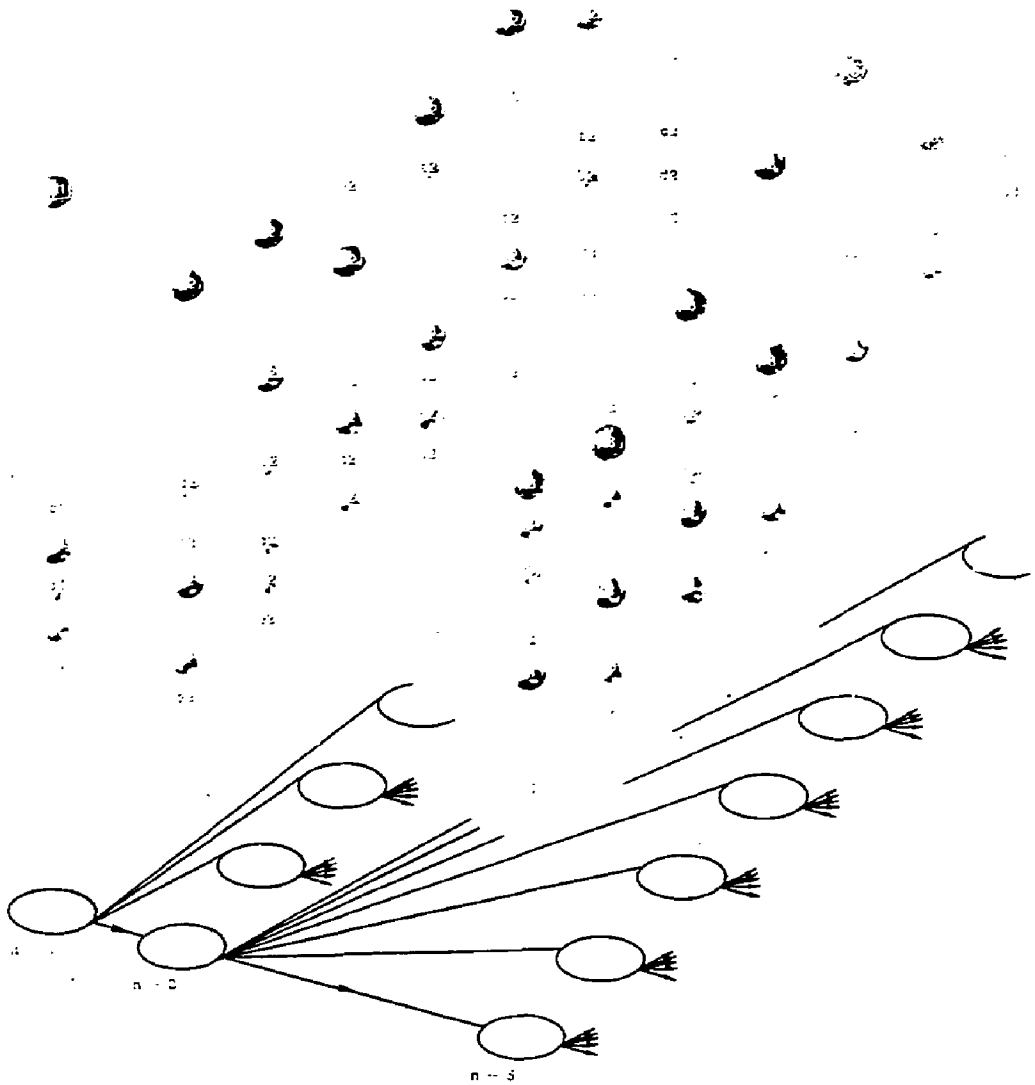

Fig. 5

Representation in energy space of multiple nucleon-nucleon scattering within a target nucleus. In the initial configuration, n = 1 because there is only one exciton, the projectile nucleon P1. P1 is equally likely to scatter from any of the fermions in the ucleus, giving rise to many n = 3 configurations (two excitons, one hole). A second scattering in any of these configurations produces an n = 5 configuration (third row), and so forth, until the system reaches equilibrium. The mathematical treatment greatly simplifies this complex series of possible events by considering only probability functions and by lumping together energetically equivalent states.

A major advance occurred when it was realized that the geometrical representation was unnecessary.[2] Rather, the nucleon trajectories could be replaced with simple energy-partition functions and the reaction could be followed in an energy space rather than a geometric space. Figure 5, which represents several possible scattering events initiated by an incident nucleon, illustrates this concept of energy space.

This approach helped explain the shape of the nonequilibrium component of the emission spectrum. Unfortunately, it could not be used, as originally formulated, to calculate absolute yields (and thus to fully test the model) because the early formulation provided no basis for determining the absolute rates of particle emission nor for verifying the correctness of the energy-partition expressions. Later work, however, used the principle of time reversal to estimate, for each hierarchy of configurations, the absolute rate of emission of nucleons.[11] This led to a formulation that satisfactorily predicted absolute spectral yields for these nonequilibrium or "precompound" reactions. Refinements of this formulation permitted the inclusion of influences from the diffuse nuclear surface, which yielded a model that produced good results over a reasonably broad range of energies.[12,13]

The precompound decay formulation was incorporated into a code for equilibrium evaporation and fission decay so that these three major components of a reaction could be calculated simultaneously.[14] We recently improved and extended the precompound formulation to permit application over a much broader dynamic range of projectile energies than could be correctly treated in earlier versions.[15]

Early data from LLNL[16] were used by Laboratory scientists as a critical test of this model. The data provided the best verification to that time of the model's predictive value over a broad range of projectile energy and target mass.

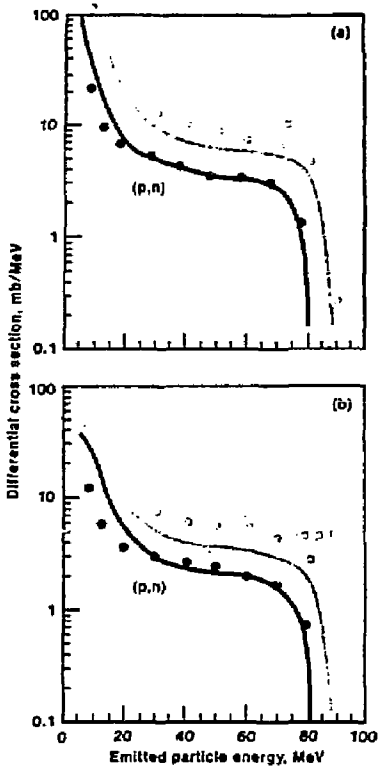

Fig. 6

Calculated and experimental (p,p') and (p,n) spectra for 90-MeV protons impinging on (a) nickel-58 and (b) aluminum-27 nuclei. Data points are experimental yields (see Ref. 6). The solid lines are the predicted precompound plus compound spectra from the ALICE/LIVERMORE 82 code (Ref. 15).

Nonequilibrium Decay Models

In Fig. 2, we compare experimental results with the results of a calculation (using this code)[15] of the niobium-93 (n,n') spectrum induced by 14-MeV neutrons. In Fig. 6, we show the result of the same kind of calculation for reactions induced by 90-MeV protons.[17] The same formulation has given excellent predictions for product yields for interactions of protons of up to 164 MeV with nickel isotopes and for yields of photonuclear and pi-minus-(π^-) induced reactions.[18,19] All these calculations were performed with the code ALICE/LIVERMORE 82.[15] These simple multiple scattering models seem to have captured the essential physics of the reaction mechanism quite well, giving us confidence in their usefulness

as tools for interpolation and extrapolation in present and future calculations of nuclear cross sections.

The same concepts that were applied to solve the problem of nucleon emission from precompound nuclei may be applied, with some additional considerations, to alpha-emission reactions induced by nucleons. Figure 7 shows the results of such a calculation for proton-induced (p,α) reactions on iron-54, -56, and -57.[20] Again, we use protons (because their incident energy is easier to control and more intense beams are available than for neutrons) to help us determine the necessary parameters of the model. Once this is done, the calculation may be used with considerable success to predict (n,α) reactions as well.[21]

We continue to improve our precompound decay models so they can be used for global predictions of nuclear cross sections. We are endeavoring at present to incorporate some aspects of the nuclear structure (nonuniform aspects of nucleon momenta in the nucleus) of individual target nuclides into the model. Experiments to test the feasibility of incorporating these details are now under way at our Cyclograaff accelerator. This refinement may make the model useful for higher particle-emission energies where the energies of a few low-lying excited states influence the emission spectrum.

Another likely use for precompound decay models is in analyzing the energy dependence of fission versus particle-emission probabilities in actinide targets. Earlier analyses that neglected precompound decay processes assumed incorrectly high excitations for the fissioning species and, therefore, may have led to an incorrect deduction of the energy dependence of the fission probability. A new analysis of these data that includes precompound effects[22] should give us more accurate fission-to-neutron-emission ratios, a matter of potential importance to reactor and weapon programs.

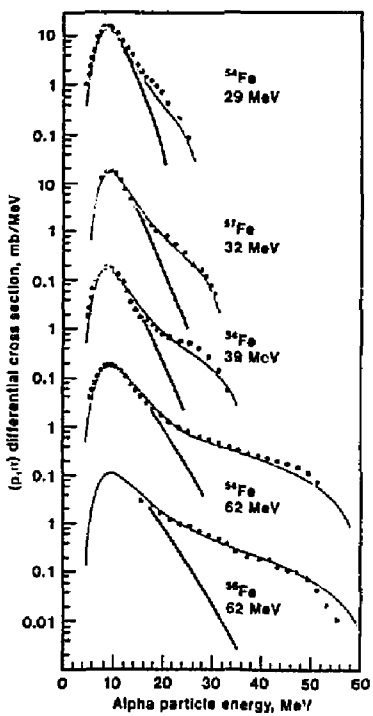

Fig. 7

Angle-integrated alpha-particle energy spectra for reactions induced by protons of different energies on iron-54, -56, and -57. Solid points are experimental results; black curves are the evaporation-model calculations, normalized to the experimental results; yellow curves are the sums of the contributions from the evaporation and the best-fitting nucleon-alpha-scattering (precompound) models. References to data and source of figure may be found in Ref. 20.

Conclusion

Models of the way nuclei decay that include a mechanism of precompound-nucleus decay have successfully predicted important nuclear-reaction cross sections. Active experimental programs at the LLNL Cyclograaff accelerator, coupled with continuing refinements of the modeling approach, should extend the value of these models still further.

Key Words: ALICE/LIVERMORE 82 (code); evaporation model; nuclear modeling; precompound model; nonequilibrium nuclear effects.

Notes and References

1. A broader review of the field of nuclear modeling appeared in *Energy and Technology Review*, May 1979 (UCRL-52000-79-5), p. 1.
2. J. J. Griffin, *Phys. Rev. Lett.* 17, 478 (1966); *Phys. Lett.* B24, 5 (1967).
3. N. Bohr, *Phys. Rev.* 53, 295 (1937).
4. V. F. Weisskopf, *Phys. Rev.*, 52, 295 (1937); and V. F. Weisskopf and D. H. Ewing, *Phys. Rev.* 57, 472 (1940).

BUDGET AND FUNDING SOURCE

In the following table budgeted costs are given in thousands of dollars ($... K); these figures are for the 1984 fiscal year (FY84), which does not completely coincide with the report period covered in this report.

Most of the funding of the E-Division Research is provided by the Division of Military Applications (DMA) of the Department of Energy (DOE). Other sources of funds from DOE are the Office of Fusion Energy (OFE), Basic Energy Sciences (BES), and Nuclear Physics Research (NP). There are additional small projects including one supported by the U.S. Navy (USN).

Since February 1982 the operations of RTNS-II have been supported in part by the government of Japan. This support amounts to about $2000 K per year and is in addition to the $2000 K shown in the following table.

AREA OF RESEARCH	SOURCE OF FUNDS	$K
Nuclear Physics (including Astrophysics)	DOE-DMA	3200
Atomic and Plasma Physics	DOE-DMA	1500
Channeling and Transition Radiation	DOE-DMA	530
Slow Positrons	DOE-DMA	850
Microwave Air Breakdown	DOE-DMA	270
Hydrogen and Helium Production	DOE-BES	210
Plasma Diagnostics	DOE-OFE	200
Electron Scattering	DOE-NP	100
Radiation Damage (RTNS-II)	DOE-OFE	2200
Decompression Sickness	USN	30

5. W. Hauser and H. Feshbach, *Phys. Rev.* **87**, 366 (1952).
6. References to the sources of data used in this figure are to be found in M. Blann and H. Vonach, Lawrence Livermore National Laboratory, Rept. UCRL-88540 (1983).
7. Pulsed sphere measurements were described in *Energy and Technology Review*, February 1978 (UCRL-52000-78-2), p. 9.
8. H. F. Lutz and J. D. Anderson, *Neutron Cross Sections Inferred from Charged Particle Data*, Lawrence Livermore National Laboratory, Rept. UCRL-14568 (1966). See also J. D. Anderson and H. F. Lutz, *Fast Neutron Cross Sections Inferred from Charged Particle Data and from the Application of Nuclear Models*, Lawrence Livermore National Laboratory, Rept. UCRL-14955 (1966).
9. Data from F. E. Bertrand, R. W. Peelle, *Phys. Rev. C* **8**, 1045 (1973).
10. K. Chen, G. Friedlander, and J. M. Miller, *Phys. Rev.* **176** (1968).
11. M. Blann, *Phys. Rev. Lett.* **27**, 337 (1971).
12. M. Blann, *Phys. Rev. Lett.* **28**, 757 (1972); M. Blann, *Nucl. Phys.* **A207**, 619 (1973).
13. M. Blann, *Ann. Rev. Nuc. Sci.* **25**, 123 (1975).
14. M. Blann, *Overlaid ALICE, A Statistical Model Computer Code Including Fission and Precquilibrium Models*, University of Rochester, Rept. COO-3494-29 (1976).
15. M. Blann and J. Bisplinghoff, *ALICE/LIVERMORE 82*, Lawrence Livermore National Laboratory, Rept. UCID-19614 (1983).
16. S. M. Grimes, J. D. Anderson, J. C. Davis, and C. Wong, *Phys. Rev. C* **8**, 1970 (1973); S. M. Grimes, J. D. Anderson, and C. Wong, *Phys. Rev. C* **13**, 2224 (1976).
17. M. Blann and H. Vonach, Lawrence Livermore National Laboratory, Rept. UCRL-88540; *Phys. Rev. C* (1983) (in press); data on (p,n) reactions are from A. M. Kalend, *Phys. Rev. C* **28**, 105 (1983), and (p,p') data are from J. R. Wu, C. C. Chang, and H. D. Holmgren, *Phys. Rev. C* **19**, 698 (1979).
18. M. Blann, *Precompound Analyses of Spectra and Yields Following Nuclear Capture of Stopped* π^-, Lawrence Livermore National Laboratory, Rept. UCRL-88737 (1983).
19. M. Blann, B. L. Berman, and T. A. Komoto, *Precompound Analysis of Photonuclear Reaction Yields*, Lawrence Livermore National Laboratory, Rept. UCRL-89348 (1983), *Phys. Rev. C* (1983) (in press).
20. A. Mignerey, M. Blann, and W. Scobel, *Nucl Phys.* **A273**, 125 (1976); W. Scobel, M. Blann, and A. Mignerey, *Nucl. Phys.* **A287**, 301 (1977).
21. P. Plischke, W. Scobel, and M. Bormann, *Z. Physik* **A281**, 245 (1977).
22. M. Blann and T. A. Komoto, *Precompound Evaporation Analyses of Excitation Functions for (α,xn) Reactions*, Lawrence Livermore National Laboratory, Rept. UCRL-89346 (1983).